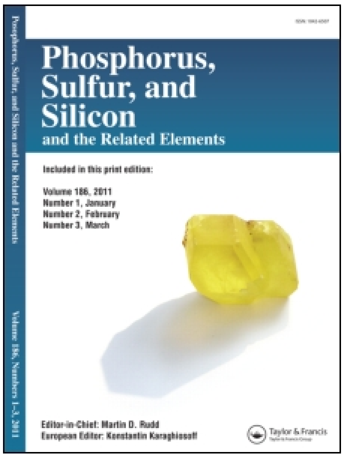

Phosphorus, Sulfur, and Silicon and the Related Elements
Publication details, including instructions for authors and subscription information:
http://www.informaworld.com/smpp/title~content=t713618290

CYCLIC PENTAOXY SILICONATES[1,2]

Robert R. Holmes[a]; Roberta O. Day[a]; Jeffrey S. Payne[a]
[a] Department of Chemistry, University of Massachusetts, Amherst, MA

To cite this Article Holmes, Robert R. , Day, Roberta O. and Payne, Jeffrey S.(1989) 'CYCLIC PENTAOXY SILICONATES[1,2]', Phosphorus, Sulfur, and Silicon and the Related Elements, 42: 1, 1 — 13

To link to this Article: DOI: 10.1080/10426508908054870

URL: http://dx.doi.org/10.1080/10426508908054870

Phosphorus, Sulfur, and Silicon, 1989, Vol. 42, pp. 1–13
Reprints available directly from the publisher
Photocopying permitted by license only

CYCLIC PENTAOXY SILICONATES[1,2]

ROBERT R. HOLMES,† ROBERTA O. DAY and JEFFREY S. PAYNE[3]
Department of Chemistry, University of Massachusetts, Amherst, MA 01003

(Received 1 December, 1988; in final form December 16, 1988)

Spirocyclic pentaoxy anionic silicates are synthesized and their molecular structures determined by X-ray diffraction. The K, 18-crown-6 salt of $[(OCMe_2CMe_2O)_2SiO\text{-}t\text{-}Bu]$ (**1**), formed from the reaction of the bis-pinacol spirosilicate and potassium *t*-butoxide, represents a new substance. Both the butylammonium salts, $[(OCMe_2CMe_2O)_2SiOR][n\text{-}BuNH_3]$ $R = OEt$ (**2**); $R = OMe$ (**3**), have structures considerably displaced from a trigonal bipyramid toward a rectangular pyramid, 38.9% for **2** and 71.2% for **3**, compared to 24.1% for **1**. Hydrogen bonding is implicated in accounting for the greater structural displacement of **2** and **3**. These pentaoxy derivatives represent the first members of this class that have been structurally characterized. Comparisons with related five-coordinated silicon and phosphorus compounds support their use as models in nucleophilic substitution reactions.

Key words: Spirocyclic; pentaoxy anionic siliconates; X-ray structures; pinacol; trigonal bipyramid; rectangular pyramid.

INTRODUCTION

Structural characterization of five-coordinated silicon compounds[4] has lagged relative to this field for phosphoranes.[4,5] Recent work in our laboratory[6–10] has demonstrated that the X-ray structures of anionic siliconates span a range from the ideal trigonal bipyramid to the square pyramid, similar to that observed earlier for the isoelectronic pentacoordinated phosphorus compounds.[4,5] A majority of compounds in each of these series contains cyclic components in which variation in their constitution provided factors favoring the degree to which the structure was displaced between idealized forms.

In both series, a dominant factor favoring the square or rectangular pyramid (RP) is the presence of two unsaturated five-membered rings containing like atoms bound to the central atom in each of the rings.[4,5b,7,8] Lesser factors are the presence of electron withdrawing ring substituents, Z, and a sterically large acyclic ligand, R, of low electronegativity in the fifth position,[7–9] e.g.,

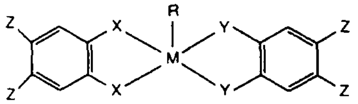

For the anionic siliconates, occasionally lattice effects[10] or intermolecular hydrogen bonding[6,8] influence the expected structural distortion based on the above factors.

These hypervalent phosphorus[11,12] and silicon[7,12–14] species provide useful models for activated states and intermediates in mechanisms of nucleophilic

---

† Author to whom all correspondence should be addressed.

displacement reactions. Recent work by Corriu and coworkers[15–17] has provided much of the current experimental basis for silicon reactions to which such models have been applied. One current application of interest concerns the role of five-coordinated anionic siliconates as intermediates in the initial stages of hydrolysis of silicic acid as it pertains to the sol-gel process for the production of ceramic silica materials.[18] In this hydrolytic sequence, the presence of pentaoxy siliconate species most likely are involved.

Toward this end as well as to extend the range of anionic siliconates for structural comparison, we have pursued synthesis, following Frye's[19] earlier work, to obtain pentaoxy siliconates. Reported here are the spirobis pinacolate deriatives, $[(Me_4C_2O_2)_2SiO\text{-}t\text{-}Bu][K,18\text{-}c\text{-}6]$, **1**, $[(Me_4C_2O_2)_2SiOEt][n\text{-}BuNH_3]$, **2**, and $[(Me_4C_2O_2)_2Si\text{-}OMe][n\text{-}BuNH_3]\cdot CH_3OH$, **3**. The *t*-butoxy derivative, **1**, represents a new compound. Frye[19] formed the diamine salt, $[(Me_4C_2O_2)_2SiOEt]_2[H_3N(CH_2)_6NH_3]$, closely related to **2**. In addition, he prepared **3** and the corresponding amine salt, $[(Me_4C_2O_2)_2SiOMe][Et_3NH]$. The molecular structures of **1–3** obtained by X-ray diffraction also are reported here.

This study provides the first structural characterization of cyclic pentaoxy siliconates and suggests that a similar study of the more easily hydrolyzable acyclic pentaoxy siliconates that closely model proposed intermediates in the sol-gel process may be possible.

RESULTS

The atom-labeling scheme for the anion of **1** is given in the ORTEP plot of Figure 1. Atom coordinates for **1** are given in Table I and selected bond lengths and

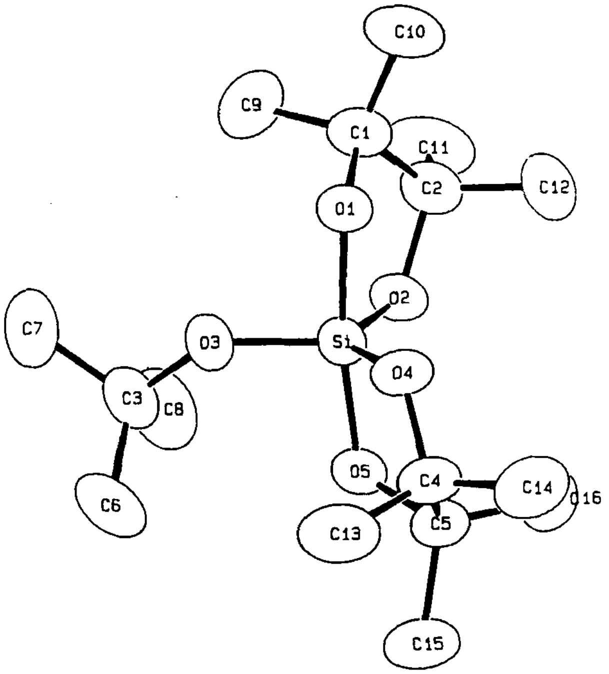

FIGURE 1 ORTEP plot of the anion in $[(Me_4C_2O_2)_2SiO\text{-}t\text{-}Bu][K,18\text{-}c\text{-}6]$, **1**, with thermal ellipsoids at the 50% probability level. Hydrogen atoms are omitted for clarity.

TABLE I

Atomic coordinates in crystalline $[(Me_4C_2O_2)_2SiO\text{-}t\text{-}Bu][K, 18\text{-}c\text{-}6]$, **1**[a]

Atom[b]	x	y	z	B equiv[c]
K	0.24672(6)	0.6546(1)	0.41813(5)	4.58(3)
Si	0.73555(7)	0.2037(1)	0.90620(6)	3.28(3)
O1	0.7745(2)	0.0837(3)	0.9717(1)	3.43(7)
O2	0.7091(2)	0.0794(3)	0.8491(1)	3.67(7)
O3	0.8295(2)	0.2675(3)	0.9263(2)	4.48(8)
O4	0.6812(2)	0.2615(3)	0.9511(1)	3.78(7)
O5	0.6821(2)	0.3161(3)	0.8422(1)	3.70(7)
O6	0.0810(2)	0.7941(4)	0.3595(2)	7.1(1)
O7	0.0870(2)	0.5247(4)	0.3444(2)	7.4(1)
O8	0.2153(3)	0.4237(5)	0.3245(2)	11.8(1)
O9	0.3765(2)	0.5222(5)	0.4023(2)	9.5(1)
O10	0.3614(3)	0.7958(5)	0.3762(2)	11.2(1)
O11	0.2232(3)	0.9186(5)	0.3674(2)	10.6(1)
C1	0.7885(3)	−0.0405(4)	0.9483(2)	4.4(1)
C2	0.7204(3)	−0.0518(4)	0.8763(2)	4.1(1)
C3	0.8690(3)	0.3377(5)	0.8901(3)	5.4(1)
C4	0.6276(3)	0.3710(4)	0.9221(2)	4.0(1)
C5	0.6076(3)	0.3599(4)	0.8449(2)	3.9(1)
C6	0.8495(3)	0.4847(5)	0.8873(3)	7.5(2)
C7	0.9621(3)	0.3158(6)	0.9309(4)	8.7(2)
C8	0.8435(3)	0.2823(6)	0.8186(3)	7.3(2)
C9	0.8748(3)	−0.0413(6)	0.9458(3)	6.7(2)
C10	0.7878(3)	−0.1481(5)	0.9969(2)	5.9(1)
C11	0.7365(4)	−0.1442(5)	0.8276(3)	6.9(2)
C12	0.6372(3)	−0.0914(5)	0.8799(3)	6.2(2)
C13	0.6747(3)	0.4972(5)	0.9536(3)	6.2(2)
C14	0.5526(3)	0.3589(6)	0.9399(2)	6.0(1)
C15	0.5827(3)	0.4927(5)	0.8071(2)	5.5(1)
C16	0.5391(3)	0.2598(5)	0.8090(2)	5.1(1)
C17	0.0392(3)	0.7058(6)	0.3855(3)	8.4(2)
C18	0.0157(3)	0.5909(6)	0.3394(3)	8.9(2)
C19	0.0749(4)	0.4310(7)	0.2941(3)	11.3(3)
C20	0.1445(5)	0.3624(7)	0.3012(4)	11.0(3)
C21	0.2878(4)	0.3590(7)	0.3348(4)	12.6(3)
C22	0.3575(4)	0.4419(8)	0.3453(4)	14.4(3)
C23	0.4423(4)	0.6076(8)	0.4154(4)	13.3(3)
C24	0.4247(4)	0.7228(9)	0.3694(4)	13.7(3)
C25	0.3284(4)	0.8989(8)	0.3290(3)	13.8(2)
C26	0.2674(7)	0.973(1)	0.3392(4)	19.8(4)
C27	0.1560(4)	0.9925(6)	0.3710(4)	11.3(3)
C28	0.1125(4)	0.9047(6)	0.4032(3)	8.9(2)

[a] Numbers in parentheses are estimated standard deviations.

[b] Atoms are labeled to agree with Figure 1.

[c] Equivalent isotropic thermal parameters are calculated as $(4/3)[a^2\beta_{11} + b^2\beta_{22} + c^2\beta_{33} + ab(\cos\gamma)\beta_{12} + ac(\cos\beta)\beta_{13} + bc(\cos\alpha)\beta_{23}]$.

angles are listed in Table II. The corresponding material for **2** is given in Figure 2 and Tables III and IV. The atom-labeling for the anion of **3** is given in the ORTEP plot of Figure 3 and hydrogen bonding interactions for **3** are illustrated in Figure 4. Atom coordinates for **3** are listed in Table V and selected bond lengths and angles are given in Table VI.

TABLE II

Selected distances (Å) and angles (deg) for [(Me$_4$C$_2$O$_2$)$_2$SiO-*t*-Bu][K, 18-c-6], **1**.[a]

Atom 1	Atom 2	Distance	Atom 1	Atom 2	Distance
Si	O1	1.777(3)	Si	O5	1.744(3)
Si	O2	1.689(3)	K	O1′	2.641(3)
Si	O3	1.670(3)	K	O4′	2.797(3)
Si	O4	1.714(4)			

Atom 1	Atom 2	Atom 3	Angle	Atom 1	Atom 2	Atom 3	Angle
O1	Si	O2	88.4(1)	O2	Si	O4	127.6(2)
O1	Si	O3	91.7(1)	O2	Si	O5	90.5(1)
O1	Si	O4	85.1(1)	O3	Si	O4	116.5(2)
O1	Si	O5	170.9(2)	O3	Si	O5	96.9(1)
O2	Si	O3	115.7(2)	O4	Si	O5	88.4(1)

[a] Estimated standard deviations in parentheses. The atom labeling scheme is shown in Figure 1.

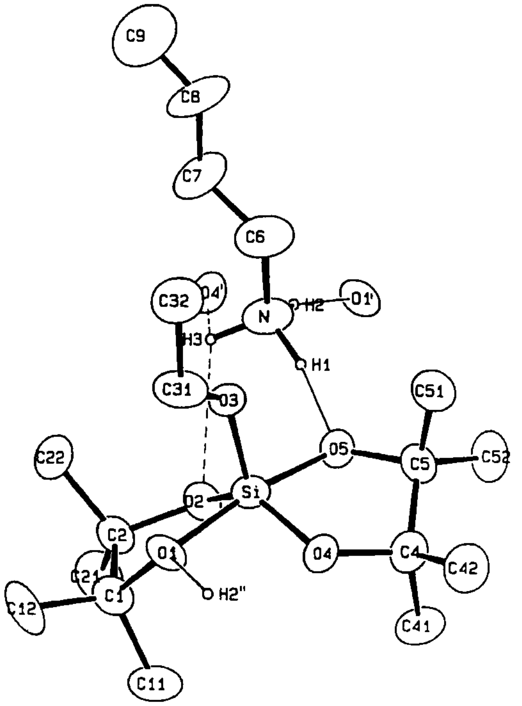

FIGURE 2 ORTEP plot of [(Me$_4$C$_2$O$_2$)$_2$SiOEt][*n*-BuNH$_3$], **2**, with thermal ellipsoids at the 30% probability level. Only amine hydrogen atoms are shown for clarity. A symmetry related O1′, O4′ ($' = x - \frac{1}{2}, \frac{1}{2} - y, 1 - z$) and a symmetry related H2″ ($'' = \frac{1}{2} + x, \frac{1}{2} - y, 1 - z$) are included. Hydrogen bonding interactions are shown as narrow lines. The van der Waals' contact between H3 and O2 and O4′ is indicated by dashed lines.

TABLE III

Atomic Coordinates in Crystalline $[(Me_4C_2O_2)_2SiOEt][n\text{-}BuNH_3]$, **2**.[a]

Atom[b]	x	y	z	B equiv[c]
Si	0.2188(2)	0.2334(1)	0.5232(1)	4.01(5)
O1	0.3021(3)	0.2708(2)	0.5862(2)	4.2(1)
O2	0.1160(3)	0.2655(2)	0.5682(2)	4.3(1)
O3	0.2541(4)	0.2849(2)	0.4573(2)	4.5(1)
O4	0.2903(3)	0.1585(2)	0.5285(2)	4.5(1)
O5	0.1261(4)	0.1871(2)	0.4741(2)	4.3(1)
N	−0.0028(4)	0.2885(3)	0.4275(3)	5.5(2)
C1	0.2506(6)	0.2932(4)	0.6484(3)	4.9(2)
C2	0.1412(6)	0.3149(4)	0.6226(3)	4.1(2)
C4	0.2416(6)	0.0958(4)	0.5016(3)	5.2(2)
C5	0.1645(6)	0.1224(4)	0.4462(3)	5.0(2)
C6	0.0432(7)	0.3204(4)	0.3621(4)	7.8(3)
C7	0.0069(7)	0.3899(4)	0.3489(5)	9.0(3)
C8	0.053(1)	0.4209(5)	0.2819(5)	12.7(4)
C9	0.019(1)	0.4835(6)	0.2639(6)	18.3(5)
C11	0.2448(7)	0.2300(4)	0.6979(3)	7.0(2)
C12	0.3149(6)	0.3519(4)	0.6806(4)	7.3(3)
C21	0.0543(7)	0.3114(4)	0.6759(4)	7.1(3)
C22	0.1401(7)	0.3891(4)	0.5891(4)	6.8(2)
C31	0.3478(7)	0.3221(4)	0.4505(4)	7.4(2)
C32	0.3589(7)	0.3577(4)	0.3849(4)	8.2(3)
C41	0.1828(6)	0.0602(4)	0.5629(4)	6.9(2)
C42	0.3286(6)	0.0479(4)	0.4754(4)	7.0(2)
C51	0.2206(7)	0.1390(4)	0.3758(4)	7.2(3)
C52	0.0713(7)	0.0750(4)	0.4307(4)	7.4(3)

[a] Numbers in parentheses are estimated standard deviations.

[b] Atoms are labeled to agree with Figure 2.

[c] Equivalent isotropic thermal parameters are calculated as (4/3) $[a^2\beta_{11} + b^2\beta_{22} + c^2\beta_{33} + ab(\cos\gamma)\beta_{12} + ac(\cos\beta)\beta_{13} + bc(\cos\alpha)\beta_{23}]$.

TABLE IV

Selected distances (Å) and angles (deg) for $[(Me_4C_2O_2)_2SiOEt][n\text{-}BuNH_3]$, **2**.[a]

Atom 1	Atom 2	Distance	Atom 1	Atom 2	Distance
Si	O1	1.762(4)	H1	N	0.974
Si	O2	1.688(4)	H2	O1′	1.805
Si	O3	1.661(4)	H2	N	0.964
Si	O4	1.694(5)	N	O1′	2.752(7)
Si	O5	1.751(5)	N	O5	2.690(7)
H1	O5	1.735			

Atom 1	Atom 2	Atom 3	Angle	Atom 1	Atom 2	Atom 3	Angle
O1	Si	O2	88.5(2)	O2	Si	O5	86.0(2)
O1	Si	O3	96.9(2)	O3	Si	O4	113.2(2)
O1	Si	O4	88.4(2)	O3	Si	O5	94.1(2)
O1	Si	O5	169.0(2)	O4	Si	O5	88.6(2)
O2	Si	O3	112.8(2)	O5	H1	N	165.7
O2	Si	O4	134.0(2)	O1′	H2	N	166.6

[a] Estimated standard deviations in parentheses. The atom labeling scheme is shown in Figure 2.

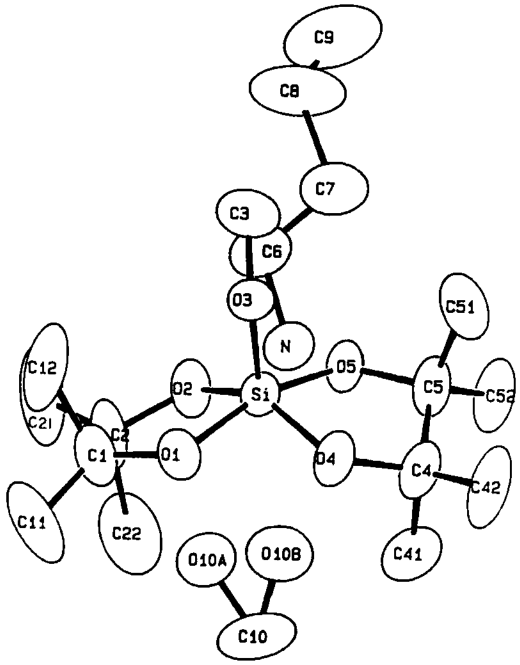

FIGURE 3 ORTEP plot of $[(Me_4C_2O_2)_2SiOMe][n\text{-}BuNH_3]\cdot CH_3OH$, **3**, with thermal ellipsoids at the 20% probability level. The two half occupied positions for 010 are shown. Hydrogen atoms are omitted for clarity.

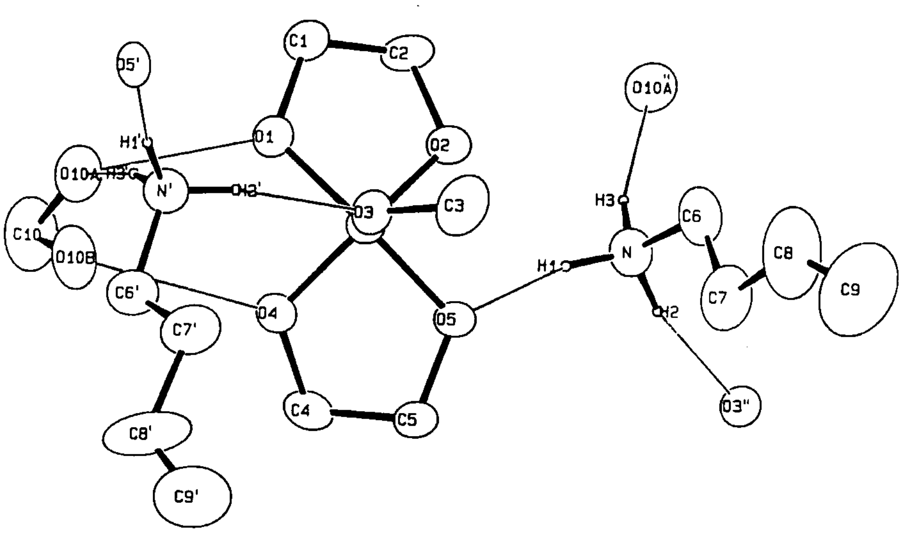

FIGURE 4 ORTEP plot showing the hydrogen bonding interactions (narrow lines) in $[(Me_4C_2O_2)_2SiOMe][n\text{-}BuNH_3]\cdot CH_3OH$.

A symmetry related cation and O5 ($' = 1.5 - x,\ \frac{1}{2} + y,\ z$) and a symmetry related O10A and O3 ($'' = 1.5 - x,\ y - \frac{1}{2},\ z$) are included. The methyl groups of the pinacol ligands and non-amine hydrogen atoms are omitted for clarity.

TABLE V

Atomic coordinates in crystalline $[(Me_4C_2O_2)_2SiOMe][n\text{-}BuNH_3]\cdot CH_3OH$, 3.[a]

Atom[b]	x	y	z	B equiv[c]
Si	0.77132(9)	0.2022(1)	0.10911(9)	4.91(4)
O1	0.7648(2)	0.2752(3)	0.1815(2)	6.6(1)
O2	0.7037(2)	0.1380(3)	0.1453(2)	6.9(1)
O3	0.7372(2)	0.2745(2)	0.0483(2)	5.6(1)
O4	0.8610(2)	0.2239(3)	0.1112(3)	7.0(1)
O5	0.7907(2)	0.1057(3)	0.0573(2)	5.7(1)
O10A	0.8670(6)	0.3904(6)	0.2259(5)	8.9(3)
O10B	0.9118(6)	0.3784(7)	0.1865(6)	10.2(3)
N	0.7012(3)	−0.0494(3)	0.0854(3)	6.7(1)
C1	0.7036(4)	0.2625(5)	0.2246(4)	8.4(2)
C2	0.6772(4)	0.1678(5)	0.2129(4)	9.2(2)
C3	0.6856(5)	0.2487(5)	−0.0025(4)	9.0(2)
C4	0.9085(3)	0.1557(5)	0.0817(4)	8.2(2)
C5	0.8615(3)	0.1058(4)	0.0268(4)	7.0(2)
C6	0.6375(4)	−0.0374(5)	0.0388(4)	8.7(2)
C7	0.6580(5)	−0.0356(6)	−0.0374(5)	11.0(3)
C8	0.5891(7)	−0.015(1)	−0.0833(6)	20.1(5)
C9	0.5766(8)	−0.051(1)	−0.1318(8)	26.4(6)
C10	0.9335(5)	0.3632(6)	0.2518(5)	12.6(3)
C11	0.7073(7)	0.3057(7)	0.2938(4)	14.8(3)
C12	0.6418(5)	0.3265(8)	0.1884(6)	18.6(4)
C21	0.6036(5)	0.1372(7)	0.2240(6)	16.1(3)
C22	0.7268(8)	0.1093(9)	0.2704(5)	23.5(4)
C41	0.9272(5)	0.0885(7)	0.1451(5)	11.4(3)
C42	0.9763(4)	0.2001(6)	0.0550(6)	12.4(3)
C51	0.8587(5)	0.1612(6)	−0.0442(4)	10.6(2)
C52	0.8826(4)	0.0064(5)	0.0103(5)	10.1(2)

[a] Numbers in parentheses are estimated standard deviations.

[b] Atoms are labeled to agree with Figure 3.

[c] Equivalent isotropic thermal parameters are calculated as $(4/3)[a^2\beta_{11} + b^2\beta_{22} + c^2\beta_{33} + ab(\cos\gamma)\beta_{12} + ac(\cos\beta)\beta_{13} + bc(\cos\alpha)\beta_{23}]$.

TABLE VI

Selected distances (Å) and angles (deg) for $[(Me_4C_2O_2)_2SiOMe][n\text{-}BuNH_3]\cdot CH_3OH$, 3.[a]

Atom 1	Atom 2	Distance	Atom 1	Atom 2	Distance
Si	O1	1.720(4)	H2	O3″	1.948
Si	O2	1.696(4)	H2	N	0.944
Si	O3	1.666(4)	H3	O10A″	2.11
Si	O4	1.685(4)	H3	N	0.958
Si	O5	1.734(4)	O10A	O1	2.65(1)
H1	O5	1.898	O10B	O4	2.80(1)
H1	N	0.952			

Atom 1	Atom 2	Atom 3	Angle	Atom 1	Atom 2	Atom 3	Angle
O1	Si	O2	88.2(2)	O3	Si	O4	105.7(2)
O1	Si	O3	97.3(2)	O3	Si	O5	101.5(2)
O1	Si	O4	86.4(2)	O4	Si	O5	87.7(2)
O1	Si	O5	161.2(2)	O5	H1	N	165.5
O2	Si	O3	109.7(2)	O3″	H2	N	164.2
O2	Si	O4	144.6(2)	O10A″	H3	N	164.6
O2	Si	O5	86.4(2)				

[a] Estimated standard deviations in parentheses. The atom labeling scheme is shown in Figure 3.

DISCUSSION

Synthesis. The spirocyclic pentaoxy anionic siliconates, **1–3**, are the first members of this class structurally characterized by X-ray diffraction analysis. The formation of **1** represents a new reaction in this area, i.e., use of the strong nucleophile combination of potassium *t*-butoxide and 18-crown-6 in reaction with the pre-formed bis-pinacol spirosilicate, Pin_2Si, Equations (1) and (2).

$$SiCl_4 + 2HOCMe_2CMe_2OH \xrightarrow{Et_2O} Si(OCMe_2CMe_2O)_2 + 4HCl \qquad (1)$$

$$\begin{aligned} &Si(OCMe_2CMe_2O)_2 + K^+O\text{-}t\text{-}Bu^- + 18\text{-}c\text{-}6 \\ &\qquad \xrightarrow{\text{toluene}} \underset{\mathbf{1}}{[(OCMe_2CMe_2O)_2SiO\text{-}t\text{-}Bu][K, 18\text{-}c\text{-}6]} \qquad (2) \end{aligned}$$

Damrauer and Danahey[20] first employed the combination of KF and 18-c-6 as a fluorinating agent in forming anionic five-coordinated organofluorosiliconates. We have prepared a number of members of this class of substances and like Damrauer found that use of the 18-c-6 cation renders considerable hydrolytic stability to these materials.

The preparations of **2** and **3** follow a procedure described by Frye[19] in his pioneering work on the synthesis and characterization of pentacoordinate silicon compounds. This involved the reaction of an alkyl ortho silicate with pinacol in the presence of a primary amine, Equation (3). This reaction is

$$\begin{aligned} &Si(OR)_4 + 2HOCMe_2CMe_2OH + n\text{-}BuNH_2 \\ &\qquad \rightarrow [(OCMe_2CMe_2O)_2SiOR][n\text{-}BuNH_3] + 3ROH \qquad (3) \\ &\qquad R = OEt\ (\mathbf{2}):\ OMe\ (\mathbf{3}) \end{aligned}$$

carried out in the absence of any added solvent as it was found that the amine provided a homogeneous reaction mixture.

In contrast to the K, 18-c-6 salt, **1**, the *n*-butylammonium salts, **2** and **3**, react rapidly with ambient moisture resulting in the formation of a glassy film on the crystals. Due to the volatility of the amine, the latter salts may revert to starting materials in the absence of a positive butylamine pressure. A similar observation of loss of amine was noted by Frye[19] in the case of the triethylammonium salt, $[(OCMe_2CMe_2O)_2SiOMe][Et_3NH]$.

Structures. The geometry about the silicon atom in all three compounds lies on the coordinate connecting a trigonal bipyramid (TBP) with O1 and O5 in axial positions to a rectangular pyramid (RP) with O3 in the apical position. Using the dihedral angle method[21] with unit vectors to assess displacement, **1** is displaced 24.1% from the TBP towards the RP, while **2** and **3** are displaced 38.9% and 71.2%, respectively. Table VII lists the "axial" (θ_{15}) and "equatorial" (θ_{24}) angles as a function of the displacement coordinate, δ_{24}. The latter varies between 53.1° for an ideal TBP to 0° for a RP. In agreement with that expected for the pseudorotational coordinate,[22] it is observed that as the axial angle θ_{15} closes down, the equatorial angle θ_{24} opens up and that these angles converge toward 150°, the trans basal angle of the RP.

TABLE VII

Pseudorotational parameters for pentaoxy anionic siliconates

Compound	θ_{15},[a] deg.	θ_{24},[b] deg.	δ_{24}(unit)[c]	%TBP→RP(unit)[d]
1	170.9(2)	127.6(2)	38.9(40.4)	24.6(24.1)
2	169.0(2)	134.0(2)	31.6(33.1)	39.3(38.9)
3	161.2(2)	144.6(2)	15.4(16.2)	71.5(71.2)

[a] θ_{15} represents the O_{ax}-Si-O_{ax} angle.

[b] θ_{24} represents O_{eq}-Si-O_{eq} angle.

[c] δ_{24} is the dihedral angle between polyhedral faces 1, 2, 4 and 2, 4, 5, where the numbers identify the atom positions.

[d] The % displacement from the TBP to the RP is calculated by a dihedral angle method described elsewhere.[21] The values in parentheses refer to the use of unit Si-O bond lengths.

In all three compounds, the longest of the Si–O bonds are to the "axial" O1 and O5 atoms, while the shortest Si—O bond is to the alkoxy oxygen atom, O3.

In the K, 18-c-6 derivative, **1**, the potassium atom is in contact with the axial O1 (2.641(3) Å) atom and the equatorial O4 (2.797(3) Å) atom. The Si–O bond lengths for these atoms are longer than the corresponding bonds to O5 and O2: Si–$O1_{ax}$ = 1.777(3) Å > Si-$O5_{ax}$ = 1.744(3) Å and Si-$O4_{eq}$ = 1.714(4) Å > Si–$O2_{eq}$ = 1.689(3) Å.

An interesting structural feature in **1** is the large value of the angle at the butoxy oxygen atom (Si–O3–C3, 134.9(2)°) which most probably reflects the steric demands of the *t*-butyl group. The corresponding angles for **2** and **3** are 127.1(4)° and 123.8(4)°, respectively.

In **2**, the cation bridges symmetry related anions via hydrogen bonds to axial O atoms and forms hydrogen bonded chains along the *a* direction. There are only two hydrogen bonds to each anion: H1····O5 = 1.735 Å and H2″····O1 = 1.805 Å. These compare to the van der Waals' sum of 2.6 Å.[23] The remaining amino hydrogen atom is in van der Waals' contact with equatorial O atoms: H3-O2 = 2.676 Å, H3–O4′ = 2.706 Å.

In **3**, the cation also bridges symmetry related anions forming hydrogen bonded chains along the *b* direction. In this case, however, the hydrogen bonds are to an axial oxygen atom (H1····O5 = 1.898 Å) and to the alkoxy O atom (H2····O3″ = 1.948 Å). The remaining amino hydrogen atom is in hydrogen bonding proximity to one of the half occupied positions of the solvate O atom (H3····O10A″ = 2.11 Å). Although H atoms were not located for the disordered solvate molecule, the proximity of O1 and O4 to the half-occupied positions for O10 suggests that further hydrogen bonding, where the OH group of the solvate is the donor, may obtain: O10A····O1 = 2.65(1) Å and O10B····O4 = 2.80(1) Å.

Thus, the progression towards the rectangular pyramid as one goes from **1** to **3** may be due to the increased number of hydrogen bonding interactions to the anions: zero for **1**, two for **2** and greater than two for **3**. Alternatively, the difference in energy between the TBP and the RP is reduced in the presence of hydrogen bonding and the shifting geometries may reflect arrangements that maximize the number of hydrogen bonding interactions possible in the solid state. The lengthening of the Si–O bonds attributable to hydrogen bonding interactions is most likely accompanied by a decrease in electron density in the effected bonds resulting in a reduction in the energy difference between the TBP and RP forms. The electron withdrawing ability of the potassium ion in **1** in causing Si–O bond lengthening apparently is weaker than that caused by hydrogen bonding interactions in **2** and **3**.

The high degree of displacement of **3** toward a rectangular pyramid is unusual. Normally derivatives containing saturated five-membered rings in pentacoordinated compounds of main group elements[4,5] are not too far displaced from the trigonal bipyramid in the absence of lattice effects. The only other anionic siliconates, outside of *this work*, containing saturated five-membered rings that show a high degree of displacement from the TBP are the dication derivatives, **4**,[24a] **5**,[9] and **6**.[24b]

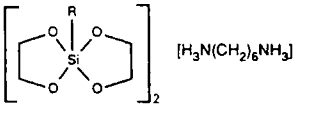

R = Me (4); Ph (5)

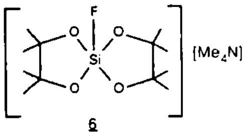

6

The displacement of **4** toward the RP is 53.3%, for **5**, 72.1%, for **6**, 53.6% and 70.8%. The latter compound has two independent molecules per unit cell[24b] and indicates the operation of lattice effects. Like that for **2** and **3** in this work, the effect is associated with the presence of hydrogen bonding.

Mechanistic Implications. The adherence of the cyclic pentaoxy siliconates, **1–3**, as well as other spirocyclic siliconates,[6–10] to the Berry pseudorotational coordinate[22] lends strong support to the existence of this type of ligand exchange process operating in nucleophilic substitution reactions of silicon proceeding with retention of configuration. Previously, the process has been applied to reactions of phosphorus compounds following retention pathways.[11] This mechanistic sequence is further strengthened by the close analogy in structural results between phosphoranes and isoelectronic anionic siliconates,[4–10] extended now to include cyclic pentaoxy siliconates. In recent theoretical studies, we have provided an underlying basis comparing the appearance of inversion and retention mechanisms in phosphorus[12] and silicon[12–14] compounds postulated to proceed via five-coordinated states.

EXPERIMENTAL

Tetrachlorosilane, tetramethoxysilane, tetraethoxysilane, pinacol, potassium *t*-butoxide, and 18-crown-6 were obtained from Aldrich Chemical Co. and used as received. *n*-Butylamine was also obtained from Aldrich Chemical Co. and was dried over sodium hydroxide prior to use. Toluene was dried over P_2O_5 and diethyl ether over sodium/benzophenone prior to use. Spirobis(pinacoloxy)-orthosilicate, $[OCMe_2CMe_2O]_2Si$, was prepared from the reaction of $SiCl_4$ with pinacol in diethyl ether solution following a previously reported method.[25]

^{1}H NMR analyses were carried out on a Varian XL 200 spectrometer. ^{29}Si NMR analyses were carried out on a Varian XL 300 spectrometer. ^{13}C NMR analyses were carried out on both instruments. ^{1}H, ^{13}C, and ^{29}Si shifts are reported relative to Me_4Si. Referencing was done externally for ^{29}Si and internally for ^{1}H and ^{13}C.

NMR spectra were obtained at room temperature, 20 ± 3°C, unless otherwise noted. Actual temperatures are believed to be within 5°C of the reported temperature. Standard experimental parameters were used to obtain the spectra. In particular, the ^{29}Si NMR spectra were obtained using a ^{13}C pulse sequence (pulse width = 8.0 Hz, D1 = 3.0 – 5.0 s).

Synthesis. (a) Potassium, 18-crown-6 Spirobis(pinacoloxy)-t-butoxy-siliconate, $[(Me_4C_2O_2)_2SiO$-*t*-$Bu][K, 18$-*c*-$6]$, *1.* To spirobis(pinacoloxy)-orthosilicate, $(Pin)_2Si$, (1.105 g, 4.25 mmol) in dry toluene (20 mL) was added potassium *t*-butoxide (0.44 g, 3.9 mmol) and 18-crown-6 (1.18 g, 4.47 mmol). The mixture was stirred for 24 h at room temperature. A slight yellow color developed. After 24 h, the mixture was filtered under nitrogen. Crystals formed upon cooling to 5°C: yield 1.04 g (42%); mp 162–180°C. ^{29}Si NMR ($CDCl_3$) −111.8 (s). Anal. Calcd for $C_{28}H_{55}KO_{11}Si$: C, 52.80; H, 9.02. Found: C, 52.98; H, 9.13.

(b) n-Butylammonium Spirobis(pinacoloxy)ethoxysiliconate, $[(Me_4C_2O_2)_2$—$SiOEt][n$-$BuNH_3]$, *2.* To a solution of pinacol (5.91 g, 50.0 mmol) in dry *n*-butylamine (50 mL) was added tetramethoxysilane (5.50 mL, 24.7 mmol). Heat was evolved. The mixture was refluxed for 10 min and then allowed to cool to room temperature. The cooled solution was stirred under an atmosphere of nitrogen. Upon further cooling to −5°C, colorless crystals formed. Crystals suitable for an X-ray diffraction study were grown from this solution held at −5°C for one week. These crystals were filtered off in a Schlenk apparatus and transferred to a glove bag. A small amount of mother liquor was maintained on the crystals to provide a positive pressure of *n*-$BuNH_2$. When the crystals were exposed to air, a glassy film developed on their surface. This surface could be physically removed by scraping to yield a fresh surface. Upon heating, an extended melting range, 50–90°C, was observed indicating decomposition: yield 4.88 g(52%). ^{29}Si NMR ($CDCl_3$) −112.1 (s). Anal. Calcd for $C_{18}H_{41}NO_5Si$: C, 56.95; H, 10.89; N, 2.69; O, 21.07. Found: 54.99; H, 10.07; N, 3.48; O, 20.29. The low carbon and hydrogen analyses are attributable to the presence of mother liquor adhering to the crystalline sample to prevent decomposition.

(c) n-Butylammonium Spirobis(pinacoloxy)methoxysiliconate·Methanol, $[(Me_4C_2O_2)_2SiOMe][n$-$BuNH_3]\cdot CH_3OH$, *3.* To a solution of pinacol (5.60 g, 47.4 mmol) in dry *n*-butylamine (50 mL) was added tetramethoxysilane (3.50 mL, 23.7 mmol). Heat was evolved upon addition. The solution was refluxed for 10 min and then allowed to cool. Stirring was stopped. After 6 h, colorless needles formed. Over time these crysals changed to large prisms. The prisms were collected, filtered in an inert atmosphere, and transferred to a glove bag. As with the ethoxy derivative, a glassy film formed on the crystals when exposed to air. The crystals were maintained with a positive pressure of mother liquor. When solvent was stripped off by washing with an organic solvent or pumping, the crystals decomposed: yield 9.42 g (82%). ^{13}C (proton decoupled) NMR ($CDCl_3$) 77.21 (s, $CHCl_3$); 72.98 (br, s, $O\mathit{C}(CH_3)_2\mathit{C}(CH_3)_2O)_2Si$); 49.50 (s, CH_3OH); 47.05 (s, $SiOCH_3$); 39.83 (s, $N\mathit{C}H_2C_3H_7$); 33.08 ($NCH_2\mathit{C}H_2C_2H_5$); 24.27 (s, $OC(\mathit{C}H_3)_2C(\mathit{C}H_3)_2O)_2Si$); 23.44 (s, $OC(\mathit{C}H_3)_2C(\mathit{C}H_3)_2O$); 18.79 (s, $NCH_2CH_2\mathit{C}H_2CH_3$); 12.49 (s, $N(CH_2)_3\mathit{C}H_3$). ^{29}Si NMR ($CDCl_3$) −111.5. Anal. Calcd for $[n$-$BuNH_3][(pin)_2SiOMe]$, $C_{18}H_{43}NO_6Si$: C, 55.85; H, 10:75; N, 3.83. Found: C, 55.88; H, 11.04; N, 3.39. The elemental analysis indicates the absence of the methanol molecule in that particular sample.

X-Ray Studies. All X-ray crystallographic studies were done using an Enraf-Nonius CAD4 diffractometer and graphite monochromated molybdenum radiation ($\lambda\ K_{\bar{\alpha}} = 0.71073$ Å) at an ambient temperature of 23 ± 2°C. Details of the experimental procedures have been described previously.[26]

Crystals were mounted in thin-walled glass capillaries which were sealed. Data were collected using the θ-2θ scan mode with $3° \leq 2\theta_{MoK\bar{\alpha}} \leq 43°$ for **1** and **3** and $3° \leq 2\theta_{MoK\bar{\alpha}} \leq 36°$ for **2**. No corrections were made for absorption. The structures were solved by use of direct methods and difference Fourier techniques, and were refined by full-matrix least-squares.[27] All computations were performed on a Microvax II computer using the Enraf-Nonius SDP system of programs.

X-ray Study for $[(Me_4C_2O_2)_2SiO$-*t*-$Bu][K, 18$-*c*-$6]$, *1.* The colorless crystal used for the X-ray study, cut from a polycrystalline mass to dimensions of 0.30 × 0.30 × 0.43 mm, diffracted poorly.

Crystal Data: $[(Me_4C_2O_2)_2SiO$-*t*-$Bu][KO_6C_{12}H_{24}]$, **1**, monoclinic space group $P2_1/c$ $[C^5_{2h} - No.\ 14]$,[28] $a = 17.673(3)$Å, $b = 10.134(2)$Å, $c = 21.487(3)$Å, $\beta = 113.60(1)°$, $Z = 4$ and $\mu_{MoK\bar{\alpha}} = 2.305\ cm^{-1}$. A total of 4029 independent reflections (+h, +k, ±l) was measured. The 41 independent non-hydrogen atoms were refined anisotropically. Hydrogen atoms were included in the refinement as fixed isotopic scatterers in idealized positions (calculated coordinates or regularized difference Fourier coordinates). The final agreement facotrs[29] were $R = 0.048$ and $R_w = 0.063$ for the 2558 reflections having $I \geq 3\ \sigma_I$.

X-ray Study for $[(Me_4C_2O_2)_2SiOEt][n$-$BuNH_3]$, *2.* Crystals of **2** are colorless, sticky laths which degrade rapidly under ambient conditions. The crystal used for the X-ray study was cut to dimensions of 0.18 × 0.25 × 0.50 mm and degraded somewhat during data collection.

Crystal Data: $[(Me_4C_2O_2)_2SiOEt][n\text{-}BuNH_3]$, **2**, orthorhombic space group Pbca [D_{2h}^{15}-No. 61],[30] $a = 12.789(4)$ Å, $b = 19.016(3)$ Å, $c = 19.200(3)$ Å, $Z = 8$ and $\mu_{MoK\bar{\alpha}} = 1.188\ cm^{-1}$. A total of 1605 independent reflections (+h, +k, +l) was measured. A decay correction was applied (relative correction factors from 1.000 to 1.091). The 25 independent non-hydrogen atoms were refined anisotropically. Hydrogen atoms were treated in the same manner described for **1**. The final agreement factors[29] were $R = 0.047$ and $R_w = 0.050$ for the 922 reflections having $I \geq 2\sigma_I$.

X-ray Study for $[(Me_4C_2O_2)_2SiOMe][n\text{-}BuNH_3]\cdot CH_3OH$, *3*. Crystals of **3** are colorless, sticky polyfaceted rods which become opaque under either ambient conditions or in a sealed capillary. The crystal used for the X-ray study was cut to dimensions of 0.50 × 0.65 × 0.65 mm and was mounted with a reservoir containing additional crystals to minimize degradation.

Crystal Data: $[(Me_4C_2O_2)_2SiOMe][n\text{-}BuNH_3]\cdot CH_3OH$, orthorhombic space group Pbca, $a = 18.449(5)$ Å, $b = 14.426(3)$ Å, $c = 18.715(4)$ Å, $Z = 8$ and $\mu_{MoK\bar{\alpha}} = 1.164\ cm^{-1}$. A total of 2852 independent reflections (+h, +k, +l) was measured. A decay correction was applied (relative correction factors from 1.000 to 1.050). Non-hydrogen atoms were refined anisotropically. Two positions were found for the methanol oxygen atom, 010, and these were included in the refinement in half occupancy for a total of 27 independent non-hydrogen atoms. Hydrogen atoms were treated as described for **1**, except that the four H atoms of the disordered MeOH molecule were omitted from the refinement. The final agreement factors[29] were $R = 0.076$ and $R_w = 0.094$ for the 1755 reflections having $I \geq 2\sigma_I$.

Note: For all three compounds, anisotropic thermal parameters, hydrogen atom parameters, and additional bond lengths and angles are deposited with the Cambridge Crystallographic Data Center (CCDC), U.K.

ACKNOWLEDGMENT

The support of this research by the National Science Foundation CHE-8504737 is gratefully acknowledged.

REFERENCES

1. (a) Pentacoordinated Molecules 75. (b) Part 74: R. O. Day, J. M. Holmes, S. Shafieezad, V. Chandrasekhar and R. R. Holmes, *J. Am. Chem. Soc.* **110,** 5377 (1988).
2. Presented in part at the Third Chemical Congress of North America, Toronto, Canada, June 1988, paper INOR 30.
3. This work represents a portion of the Ph.D. Thesis of J. S. Payne, University of Massachusetts, Amherst, MA, 1989.
4. R. R. Holmes, "Five-Coordinated Structures," in *Progress in Inorganic Chemistry,* Vol. 32, S. J. Lippard, Ed., John Wiley and Sons, New York, 119 (1984).
5. (a) R. R. Holmes, *Pentacoordinated Phosphorus—Structure and Spectroscopy,* Vol. I, ACS Monograph 175, American Chemical Society, Washington, D.C., Chapter 2 (1980). (b) R. R. Holmes, *Acc. Chem. Res.* **12,** 257 (1979).
6. R. R. Holmes, R. O. Day, V. Chandrasekhar and J. M. Holmes, *Inorg. Chem.* **24,** 2009 (1985).
7. R. R. Holmes, R. O. Day, V. Chandrasekhar, J. J. Harland, and J. M. Holmes, *Inorg. Chem.* **24,** 2016 (1985).
8. R. R. Holmes, R. O. Day, J. J. Harland, and J. M. Holmes, *Organometallics* **3,** 347 (1984).
9. R. R. Holmes, R. O. Day, J. J. Harland, A. C. Sau and J. M. Holmes, *Organometallics* **3,** 341 (1984).
10. J. J. Harland, R. O. Day, J. F. Vollano, A. C. Sau, and R. R. Holmes, *J. Am. Chem. Soc.* **103,** 5269 (1981).
11. R. R. Holmes, *Pentacoordinated Phosphorus—Reaction Mechanisms,* Vol. II, ACS Monograph 176, American Chemical Society, Washington, D.C., Chapter 2 (1980).
12. J. A. Deiters and R. R. Holmes, *J. Am. Chem. Soc.* **110,** 7672 (1988).
13. J. A. Deiters and R. R. Holmes, *J. Am. Chem. Soc.* **109,** 1686 (1987).
14. J. A. Deiters and R. R. Holmes, *J. Am. Chem. Soc.* **109,** 1692 (1987).
15. R. J. P. Corriu and C. J. Guerin, *Organomet. Chem.* **198,** 231 (1980).
16. R. J. P. Corriu and C. J. Guerin, *Adv. Organomet. Chem.* **20,** 265 (1982), and references cited therein.

17. R. J. P. Corriu, *Phosphorus and Sulfur* **27,** 1 (1986), and references cited therein.
18. (a) R. K. Iler, *The Chemistry of Silica,* John Wiley and Sons, New York (1979). (b) T. Shimono, T. Isobe, T. Tarutani, *J. Chromatogr.* **258,** 73 (1983). (c) C. Okkerse, "Porous Silica," in B. G. Linsen, Ed., *Physical and Chemical Aspects of Adsorbents and Catalysts,* Academic Press, New York, Chapter 5 (1970).
19. C. L. Frye, *J. Am. Chem. Soc.* **92,** 1205 (1970).
20. R. Damrauer and S. E. Danahey, *Organometallics* **5,** 1490 (1986).
21. R. R. Holmes and J. A. Deiters, *J. Am. Chem. Soc.* **99,** 3318 (1977).
22. R. S. Berry, *J. Chem. Phys.* **32,** 933 (1960).
23. L. Pauling, *The Nature of Chemical Bond,* 3rd ed. Cornell University Press, Ithaca, New York, 260 (1960).
24. (a) D. Schomburg, *Z. Natursforsch., B. Anorg. Chem., Org. Chem.* **37B,** 195 (1982). (b) *ibid,* **38B,** 938 (1983).
25. W. Hahn, *Makromol. Chem.* **11,** 51 (1953).
26. A. C. Sau, R. O. Day, and R. R. Holmes, *Inorg. Chem.* **20,** 3076 (1981).
27. The function minimized was $\sum w(|F_o| - |F_c|)^2$, where $w^{1/2} = 2 F_o L_p / \sigma_I$.
28. *International Tables for X-ray Crystallography*; Kynoch: Birmingham, England, 1969; Vol. I, p. 99.
29. $R = \sum ||F_o| - |F_c|| / \sum |F_o|$ and $R_w = \{\sum w(|F_o| - |F_c|)^2 / \sum w |F_o|^2\}^{1/2}$.
30. *Ref.* 28, *p.* 150.